

Contribution from the Ames Laboratory of the USAEC and the Department of Chemistry, Iowa State University, Ames, Iowa 50010

Polarized Crystal Absorption Spectra and Crystal Structure for Potassium Tetrabromoplatinate(II)

ROY F. KROENING, RHONDA M. RUSH, DON S. MARTIN, Jr.,* and JON C. CLARDY¹

Received September 12, 1973

AIC30672*

Crystals of anhydrous K_2PtBr_4 have the tetragonal K_2PtCl_4 structure, with $a = 7.350$ (1) Å and $c = 4.326$ (1) Å. The Pt-Br bond length is 2.445 (2) Å. Spectra for single crystals have been recorded at 300 and 15°K and in aqueous solution. For K_2PtBr_4 crystals the $d \leftarrow d$ transitions occur at 1500–2000 cm^{-1} lower energy than for the corresponding transitions in K_2PtCl_4 . The ratios of $a-x,y:c-z$ intensities for the $d \leftarrow d$ transitions are greater for K_2PtBr_4 than for K_2PtCl_4 . Vibrational structure at 15°K was resolved for two of the $d \leftarrow d$ bands but for no others. The ${}^1A_{2g} \leftarrow {}^1A_{1g}$ transition was identified by its absence from the c polarization spectrum. The crystal spectra indicate that intense transitions in the solution spectrum at 34,200 and 37,200 cm^{-1} must occur with $a-x,y$ polarization and the first ${}^1A_{2u}$ state cannot occur below 48,000 cm^{-1} . The two intense bands are attributed to a 1E_u state and a triplet state whose components in the E'_{1u} irreducible representation of the double group, D'_{4h} , mix with 1E_g by spin-orbit coupling. A weak transition at 30,500 cm^{-1} in both a and c polarization appears to be dipole allowed by its temperature dependence and has been assigned as 3E_u .

Introduction

Electronic spectra of the square-planar complexes of platinum(II) with $5d^8$ configuration have been studied extensively by both experimental and theoretical methods. A recent review² has summarized contributions of polarized single-crystal spectra for these systems. Such studies have permitted some transition assignments by application of vibronic and ligand field selection rules. Low-temperature spectra afforded by liquid nitrogen or helium have provided better resolution because of the narrowing of bands and in some cases have revealed vibrational structure as well. In addition, a striking decrease of intensity at low temperature has served to identify symmetry-forbidden transitions excited by a vibronic mechanism. On the other hand, a transition with a significant nonzero transition dipole is characterized by a band which grows taller as it narrows at the lower temperature.

Basch and Gray³ and Cotton and Harris⁴ have presented one-electron semiempirical MO treatments for the $PtCl_4^{2-}$ ion. Earlier, Fenske, *et al.*,⁵ and Martin, *et al.*,⁶ provided a ligand field treatment of the d^8 configuration which included the electron-electron repulsions as well as spin-orbit coupling.

Low-temperature spectra for K_2PtCl_4 have been reported by Martin, *et al.*,⁷ by Mortensen,⁸ and more recently by Patterson, *et al.*⁹ The latter workers also prepared dilute solutions of Cs_2PtCl_4 in host crystals of Cs_2ZrCl_6 which provided sharper resolution of vibrational structure on the absorption bands. Their doped crystals also exhibited luminescence for one transition band with sharply resolved vibrational structure at 4°K.

The crystal structure^{10,11} for K_2PtCl_4 is optimal for spectral

studies in that the $PtCl_4^{2-}$ ions, one ion per unit cell, occupy sites with full D_{4h} symmetry so their symmetry axis is directed along the tetragonal c axis of the crystal. The spectrum for c -axis polarization accordingly provides the ion's z -axis or out-of-plane absorption, and the a -axis spectrum provides the ion's x,y -axis or in-plane absorption.

Bilman and Anderson have reported that potassium tetrabromoplatinate(II) crystallizes as $K_2PtBr_4 \cdot 2H_2O$ ¹² in dark brown to black orthorhombic crystals. Upon evaporation of solutions of K_2PtBr_4 , we have observed the formation of these crystals, which upon exposure to the laboratory atmosphere frequently underwent a crystal transformation, presumably with dehydration, to form a compact finely powdered opaque block retaining the original crystal shape. However, upon long standing with very slow dehydration, a portion of the sample formed crystals which remained indefinitely in a dry atmosphere. X-Ray diffraction of these dehydrated crystals, below, demonstrated that they were tetragonal and isomorphous with the K_2PtCl_4 . When the saturated solution was evaporated as a film between fused-silica plates at room temperature, the hydrate crystals formed first. If dried for a long time between plates so the dehydration was very slow, some anhydrous crystals were occasionally found which were suitable for spectral studies. When the film of solution between plates was evaporated at 35°, no hydrate crystals were formed, but crystals of K_2PtBr_6 and some platinum black invariably were found associated with K_2PtBr_4 crystals, so a slow autoredox reaction had occurred.

The thin crystals of K_2PtBr_4 were distinctly dichroic. In thin sections less than 30 μ thick they possessed a pale pink color with c -polarized light, and they were a pale tan in a -polarized light. With these anhydrous crystals of K_2PtBr_4 the polarized absorption spectra have been recorded to provide a very interesting comparison with those of K_2PtCl_4 .

Experimental Section

K_2PtBr_4 . A slurry of K_2PtBr_6 in water was reduced either by oxalate or by cautious addition of hydrazine. As crystals began to form upon evaporation of the resulting solution, they were withdrawn from contact with solution. It was not possible to wash the crystals because of their rapid dissolution in water. A thermogravimetric analysis of a typical freshly prepared batch of crystals following its dehydration yielded a weight loss to 650° as Br_2 of 25.6%, a weight loss to 900° as KBr of 42.6%, and a residue as Pt of 31.7% (calculated values: Br_2 , 27.0%; KBr , 40.1%; Pt, 32.9%). This

(12) E. Bilman and A. C. Anderson, *Ber. Deut. Chem. Ges.*, **36**, 1565 (1903).

(1) Camille and Henry Dreyfus Foundation Teacher-Scholar Grant Awardee, 1972–1977, and Fellow of the Alfred Sloan Foundation 1973–1975.

(2) D. S. Martin, Jr., *Inorg. Chim. Acta Rev.*, **5**, 107 (1971).

(3) H. Basch and H. B. Gray, *Inorg. Chem.*, **6**, 365 (1967).

(4) F. A. Cotton and C. B. Harris, *Inorg. Chem.*, **6**, 369 (1967).

(5) R. F. Fenske, D. S. Martin, Jr., and K. Ruedenberg, *Inorg. Chem.*, **1**, 44 (1962).

(6) D. S. Martin, M. A. Tucker, and A. J. Kassman, *Inorg. Chem.*, **5**, 1298 (1966).

(7) D. S. Martin, M. A. Tucker, and A. J. Kassman, *Inorg. Chem.*, **4**, 1682 (1965).

(8) O. S. Mortensen, *Acta Chem. Scand.*, **19**, 1500 (1965).

(9) H. H. Patterson, J. J. Godfrey, and S. M. Khan, *Inorg. Chem.*, **11**, 2872 (1972).

(10) R. G. Dickinson, *J. Amer. Chem. Soc.*, **44**, 2404 (1922).

(11) R. H. Mais, P. G. Owston, and A. M. Wood, *Acta Crystallogr., Sect. B*, **28**, 393 (1972).

analysis was consistent with a KBr impurity content of *ca.* 4%. For the solution spectrum the molar absorptivity was calculated from the platinum content of this material. Crystals for spectra were grown from aqueous solutions prepared by redissolving this material.

A determination of the indices of refraction by the Becke line immersion method revealed $n_c(n_E) = 1.5934$ and $n_a(n_O) > 1.74$ (immersion in CH_2I_2) for the Na D line, 25° . A crystal with optical quality faces containing the optic axis was found. This crystal provided well-developed periodic fluctuation in the recordings of absorbance vs. wavelength for the region of low absorption because of interference of the transmitted beam with light that suffered internal reflections. Such interference effects had served to provide the thickness and refractive indices of Magnus' green salt,¹³ $\text{Pt}(\text{NH}_3)_4\text{PtCl}_4$. However, in the present work, the treatment was modified to take account of the important variation of refractive index with wavelength. An absorbance minimum at a wavelength, λ_N , corresponds to a phase delay upon double internal reflection of $2\pi N$ where N is an integer. Successive minima at shorter wavelengths correspond to integral increases in the number of wavelengths, $N + 1, N + 2, \dots, N + m$, etc. In *c* polarization, for example, 40 absorbance minima appeared between 6200 and 4200 Å. The thickness of the crystal, L , is given by the expression

$$2L = N\lambda_N/n_N \quad (1)$$

where n_N is the index of refraction at λ_N . For successive absorbance minima therefore

$$n_m \bar{\nu}_m / n_N \bar{\nu}_N = 1 + m/N \quad (2)$$

where $\bar{\nu}_m$ is the wave number for the minima, $N + m$, etc.

The separation of successive minima either in wavelength or wave number depends upon the value N and also upon dispersion or variation of the index of refraction with wavelength. Thus if

$$n_m/n_N = 1 + \alpha(\bar{\nu}_m - \bar{\nu}_N) + \beta(\bar{\nu}_m + \bar{\nu}_N)^2 \quad (3)$$

it can be shown from eq 2 that

$$m\bar{\nu}_N/(\bar{\nu}_m - \bar{\nu}_N) = N(1 + \alpha\bar{\nu}_N) + N(\alpha\bar{\nu}_N + \beta\bar{\nu}_N^2)(\bar{\nu}_m - \bar{\nu}_N)/\bar{\nu}_N + N\beta\bar{\nu}_N^2(\bar{\nu}_m - \bar{\nu}_N)^2/\bar{\nu}_N^2 \quad (4)$$

From a weighted quadratic least-squares fit ($w_i = M^2$) of $m\bar{\nu}_N/(\bar{\nu}_m - \bar{\nu}_N)$ vs. $(\bar{\nu}_m - \bar{\nu}_N)/\bar{\nu}_N$ for the *c*-polarization recording, values were $N = 63$ and $(dn_c/d\bar{\nu})/n_c = 7.8 \times 10^{-6} \text{ cm for } \bar{\nu}_N = 17,090 \text{ cm}^{-1}$ (5852 Å). The uncertainty in N , as evidenced by calculations based on different minima amounted to *ca.* 5%. From these values the thickness of this crystal was calculated to be $11.5 \pm 0.5 \mu$.

From this thickness and the interference for *a* polarization, the value of $n_a(n_O)$ was calculated to be 1.95. This value contains the 5% uncertainty arising from the uncertainty in thickness. However, it does confirm the observation of the Becke line under CH_2I_2 immersion. Such a high index of refraction for n_a in comparison to n_c or n_o for K_2PtCl_4 may result from the proximity of strong absorption bands in *a* polarization for K_2PtBr_4 .

Thicknesses of other crystals were inferred from the ratios of absorbances of one of their peaks to the corresponding peak of this crystal.

Crystal Structure Determination. A short section of a square needle crystal of K_2PtBr_4 was mounted on a glass fiber for diffraction studies. Preliminary precession photographs indicated a primitive tetragonal unit cell for which no systematic absences were observed. These facts suggested the space group $P4/mmm$ (D_{4h}^1 , No. 123) and indicated that K_2PtBr_4 is isomorphous with K_2PtCl_4 .^{10,11} The crystal data for K_2PtBr_4 indicate $\alpha = \beta = \gamma = 90^\circ$; $a = b = 7.350$ (1) Å, $c = 4.326$ (1) Å, $Z = 1$ molecule/cell, $d_{\text{calcd}} = 4.191 \text{ g/cm}^3$, and mol wt 592.93.

A crystal $0.1 \times 0.1 \times 0.2 \text{ mm}$ was used for data collection at room temperature by a four-circle automated diffractometer equipped with a graphite monochromator and a scintillation counter. Data were collected with Mo K α radiation within a 2θ sphere of 60° over two octants. A total of 727 reflections were measured by means of θ - 2θ scans. Three standard noncoplanar reflections were measured periodically to confirm that no detectable crystal decomposition occurred during the data collection. Equivalent reflections were averaged and 241 unique reflections utilized in the data work-up. Intensity data

were corrected for Lorentz-polarization effects and absorption with a linear absorption coefficient.¹⁴ The F_o^2 were calculated and 13 reflections for which F_o^2 were less than 3σ were considered to be unobserved and were omitted from the refinement.

Three-dimensional Patterson maps constructed from sharpened data confirmed the K_2PtCl_4 structure with the Pt atom at the special position (0, 0, 0) the K atom at $(\pm 1/2, 0, \pm 1/2)$ and $(0, \pm 1/2, \pm 1/2)$ and the four bromide atoms at $(\pm x, \pm x, 0)$. For refinements scattering factors from Hanson, *et al.*,¹⁵ were employed. Anisotropic temperature factors were restricted under the symmetry requirements in accordance with the following relationships:¹⁶ for Pt and K

$$\beta_{11} = \beta_{22} \neq \beta_{33}, \quad \beta_{12} = \beta_{23} = \beta_{13} = 0 \quad (5)$$

for Br

$$\beta_{11} = \beta_{22} \neq \beta_{33}, \quad \beta_{12} \neq 0, \quad \beta_{13} = \beta_{23} = 0 \quad (6)$$

Thus, refinement was required for only one positional parameter, x , and seven temperature factors. The refinement was accomplished by full-matrix least squares to a conventional discrepancy factor of R , $\Sigma|F_o| - |F_c|/\Sigma|F_o| = 0.094$.¹⁷ The structural parameters and indicated interatomic distances are included in Table I. The Pt-Br distance is 0.129 (3) Å greater than the Pt-Cl and the Pt-Pt distance is 0.182 (2) Å greater in K_2PtBr_4 than in K_2PtCl_4 as a reasonable consequence of the larger covalent and van der Waals radii of bromine.

Spectra. The techniques for recording polarized spectra have been described previously.² In the cryostat a metal plate, to which the crystal was attached through a bond of varnish or silicone grease, was pressed against a copper block which formed the bottom of the liquid helium can. It was assumed to provide a nominal 15°K for the crystal.

Spectra of solutions were recorded by the Cary 14 spectrophotometer. A solution of standard K_2PtBr_4 was prepared from a weighed sample of the analyzed dehydrated salt in 1 *M* KBr. This solution was diluted quantitatively with 1 *M* KBr for the regions of high intensity. The spectrum in Figure 1 up to $43,000 \text{ cm}^{-1}$ was recorded in this way. Beyond this point absorption by bromide became too high. Therefore, a sample of K_2PtBr_4 was dissolved in H_2O , and a recording of the remainder of the spectrum was completed within 2 min of the contact with water. The molar absorptivity of this solution was matched to the other curve at $43,000 \text{ cm}^{-1}$. It was noted that the absorbance of the solution at $48,000 \text{ cm}^{-1}$ decreased by only 3% in 5 min.

The components of the spectrum were resolved as log-normal functions by a least-squares program, LOGFIT of Siano and Metzler.¹⁸

Results and Discussion

From the previous experimental and theoretical studies for PtCl_4^{2-} the qualitative ordering in energy of the spectroscopically relevant orbitals, shown in Figure 2, is generally accepted. The connecting lines on the diagram identify the principal component of each MO. The lowest unfilled orbital is the antibonding orbital $\sigma^*(b_{1g})$, based on the $d_{x^2-y^2}$; and the highest filled orbital is b_{2g} , based on the d_{xy} and considered π antibonding. The spectra for PtBr_4^{2-} will be discussed in terms of this orbital scheme.

Aqueous Solution Spectrum. The components resolved from the aqueous solution spectrum in Figure 1 have been listed in Table II. Each of these components corresponds rather closely in energy and intensity with the components tabulated by Mason and Gray¹⁹ for acetonitrile solutions of $\{\text{N}(\text{C}_2\text{H}_5)_2\}_2\text{PtBr}_4$. The steeply rising intense absorption at high energy may represent a solvent \leftarrow ion transition. In the resolution of the spectrum, four components were introduced below $24,000 \text{ cm}^{-1}$ because the crystal spectra indicated a

(14) "International Tables for X-Ray Crystallography," Vol. III, Kynoch Press, Birmingham, England, 1952, p 157.

(15) H. P. Hanson, F. Herman, J. D. Lea, and S. Skillman, *Acta Crystallogr.*, 17, 1040 (1964).

(16) H. A. Levy, *Acta Crystallogr.*, 9, 679 (1956).

(17) See paragraph at end of paper regarding supplementary material.

(18) D. B. Siano and D. E. Metzler, *J. Chem. Phys.*, 51, 1856 (1969).

(19) W. R. Mason, III, and H. B. Gray, *J. Amer. Chem. Soc.*, 90, 5722 (1968).

(13) D. S. Martin, Jr., R. M. Rush, R. F. Kroening, and P. F. Fanwick, *Inorg. Chem.*, 12, 301 (1973).

Table I. Structural Parameters for $K_2PtBr_4^a$

Atom	x/a	y/a	z/c	β_{11}	β_{33}	β_{12}
Pt	0.0	0.0	0.0	0.01141	0.03424	
K	0.5	0.0	0.5	0.04358	0.5932	
Br	0.2352	0.2352	0.0	0.01382	0.06200	-0.00378

^a Pt-Br = 2.445 (2) Å; Pt-Pt = 4.326 (1) Å; Br-K = 3.385 (1) Å.

transition at 22,700 cm^{-1} . However, the LOGFIT program moved all four components below 21,000 cm^{-1} where they were grouped as two pairs, the members of each pair exhibiting considerable overlap. The components of each pair have been combined in Figure 1 to give the two rather unsymmetrical peaks at 17,000 and 19,900 cm^{-1} . These two peaks can be attributed to spin-forbidden $\sigma^*(b_{1g}) \leftarrow d$ transitions. The well-defined peak at 24,000 cm^{-1} and the shoulder at 27,200 cm^{-1} then correspond to spin-allowed $\sigma^*(b_{1g}) \leftarrow d$ transitions.

The transitions above 32,000 cm^{-1} appear so intense that they cannot be $d \leftarrow d$ transitions.

Crystal Spectra. $d \leftarrow d$ Transitions. The polarized crystal spectra for 300 and 15°K are presented in Figure 3. Wave numbers for band maxima, molar absorptancies, indicated oscillator strengths for 15°K, and proposed assignments for the transitions have been listed in Table II. All the transitions at lower energies than the valley at 29,000 cm^{-1} are assigned to $\sigma^*(b_{1g}) \leftarrow d$ transitions. The solution spectrum at 300°K possessed the well-resolved peak at 24,000 cm^{-1} . In the crystal at 300°K for $a-x, y$ polarization there is a shoulder at about this energy which gives a well-resolved band at 15°K that exhibits vibrational structure. The transition is completely absent in $c-z$ polarization. This feature identifies the transition as ${}^1A_{2g} \leftarrow {}^1A_{1g}$, $\sigma^*(b_{1g}) \leftarrow b_{2g}(d_{xy})$, for the vibronic selection rules require that this transition occur only in x, y polarization.⁷ This constitutes the spin-allowed transition with the lowest energy. The corresponding transition for K_2PtCl_4 has similar characteristics. The transition with the maximum at 27,400 cm^{-1} in $c-z$ polarization and 26,800 cm^{-1} in $a-x, y$ polarization is assigned as ${}^1E_g \leftarrow {}^1A_{1g}$, $\sigma^*(b_{1g}) \leftarrow e_g(d_{xz}, yz)$, by analogy with the K_2PtCl_4 spectra for which the assignment was confirmed by the presence of A terms in the MCD spectrum for the aqueous solution.^{20,21} Accordingly, the shoulder at 16,900 (c) and 17,000 cm^{-1} (a) and the bands at 18,800 (c) and 19,100 cm^{-1} (a) have been assigned as ${}^3A_{2g}$ and 3E_g . The large spin-orbit coupling for the heavy platinum atom accounts for the high intensity of these spin-forbidden transitions. There are nine states included in ${}^3A_{2g}$ and 3E_g but even at 15°K only the shoulder and peak are resolved. There is, in addition, at 15°K clearly a shoulder on the low-energy side of the ${}^1A_{2g}$ band in $a-x, y$ polarization which was not resolvable at 300°K. This shoulder also exhibits the vibrational structure and a very weak band can also be seen in $c-z$ polarization at this energy. An assignment of this transition to a ${}^3B_{1g}$, $\sigma^*(b_{1g}) \leftarrow a_{1g}(d_{z^2})$, component seems logical. With strong spin-orbit coupling the states must be described in terms of the double rotational group D'_{4h} . Patterson, *et al.*,⁹ reported that the corresponding band of $PtCl_4^{2-}$ is the one seen in luminescence of crystals of Cs_2ZrCl_6 doped with Cs_2PtCl_4 . Their analysis of the sharp vibrational lines provided evidence for assignment of this transition to the component $E'_{1g}({}^3B_{1g})$.

The region with the vibrational structure at 15°K is shown

(20) D. S. Martin, Jr., J. G. Foss, M. E. McCarville, M. A. Tucker, and A. J. Kassman, *Inorg. Chem.*, **5**, 491 (1966).

(21) A. J. McCaffery, P. N. Schatz, and P. J. Stephens, *J. Amer. Chem. Soc.*, **90**, 5730 (1968).

Table II. Transitions Observed for K_2PtBr_4 in Aqueous Solution and in Single Crystals

$\bar{\nu}$, cm^{-1}	PtBr ₄ ²⁻ aqueous soln (300°K)		K ₂ PtBr ₄ crystals (15°K)		K ₂ PtBr ₄ crystals (15°K)		Excited state: transition assignments
	ϵ_{max} , $cm^{-1}M^{-1}$	Osc str	$\bar{\nu}$, cm^{-1}	ϵ_{max} , $cm^{-1}M^{-1}$	$\bar{\nu}$, cm^{-1}	Osc str	
17,000	10	1.1×10^{-5}	16,900	1	5×10^{-6}	4×10^{-5}	${}^3A_{2g}$: $\sigma^*b_{1g}(d_{x^2-y^2}) \leftarrow b_{2g}(d_{xy})$
19,900	22	9.1×10^{-5}	18,800	12	10.7×10^{-5}	1.3×10^{-4}	3E_g : $\sigma^*b_{1g}(d_{x^2-y^2}) \leftarrow e_g(d_{xz}, yz)$
24,000	118	1.7×10^{-3}	22,600	3	1.6×10^{-5}	9.2×10^{-5}	${}^1B_{1g}$: $\sigma^*b_{1g}(d_{x^2-y^2}) \leftarrow a_{1g}(d_{z^2})$
27,200	84	9.6×10^{-4}	Absent			3.5×10^{-4}	${}^1A_{2g}$: $\sigma^*b_{1g}(d_{x^2-y^2}) \leftarrow b_{2g}(d_{xy})$
31,500	600	1.1×10^{-2}	27,400	44	4.2×10^{-4}	7.0×10^{-4}	1E_g : $\sigma^*b_{1g}(d_{x^2-y^2}) \leftarrow e_g(d_{xz}, yz)$
34,200	2,700	3.0×10^{-2}	30,500	32	1.5×10^{-4}	1.5×10^{-4}	3E_g : $\sigma^*b_{1g}(d_{x^2-y^2}) \leftarrow e_g(d_{xz}, yz)$
37,200	8,500	1.3×10^{-1}	33,800	39	2.4×10^{-4}		${}^3A_{2u}$: $a_{2u}(p_z) \leftarrow e_g(d_{xz}, yz)$; $\sigma^*b_{1g}(d_{x^2-y^2}) \leftarrow e_u(L\pi)$
48,100	11,800		35,300	15	6.2×10^{-5}		Same as above?
			Intense absorption				${}^1B_{1g}$: $\sigma^*b_{1g}(d_{x^2-y^2}) \leftarrow a_{1g}(d_{z^2})$
			Intense absorption				${}^3B_{1u}$: $a_{2u}(p_z) \leftarrow b_{2g}(d_{xy}) + {}^1E_u(E'_{1u} \text{ component})$
			Intense absorption				${}^3B_{1u}$: $a_{2u}(p_z) \leftarrow b_{2g}(d_{xy}) + {}^3B_{2u} \text{ component}$
			Intense absorption				${}^3B_{1u}(E'_{1u} \text{ component})$
							${}^1A_{2u}$: $a_{2u}(p_z) \leftarrow a_{1g}(d_{z^2})$; $\sigma^*b_{1g}(d_{x^2-y^2}) \leftarrow b_{2u}(L\pi)$

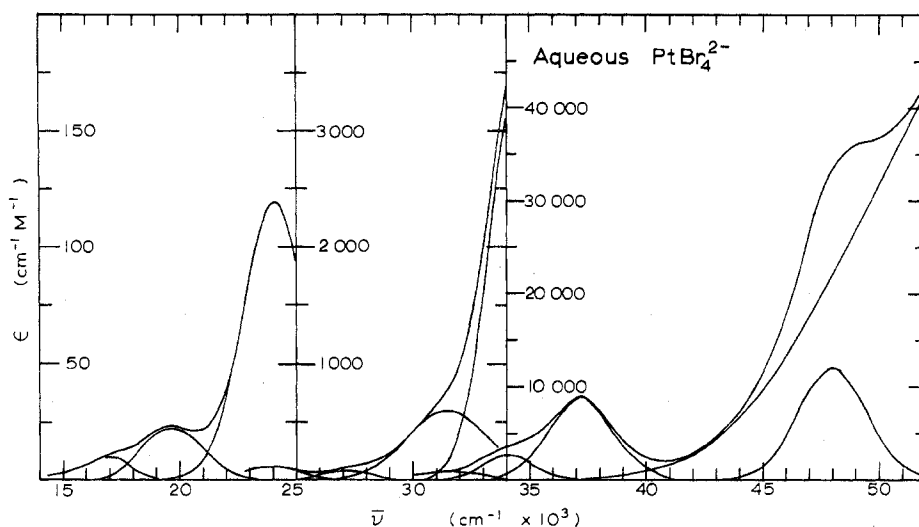


Figure 1. Spectrum of K_2PtBr_4 in aqueous solution. From 14,000 to 43,000 cm^{-1} the solution was 1 M in KBr . Above 43,000 cm^{-1} , where Br^- absorbs strongly, a dilute solution was prepared by dissolving crystals in water. The solution was introduced into the cells and recorded immediately.

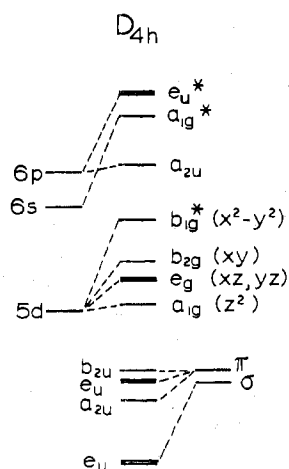


Figure 2. Molecular orbital scheme for $PtCl_4^{2-}$ and $PtBr_4^{2-}$ in D_{4h} symmetry. Only the p orbitals for halide are shown and gerade orbitals arising from the ligand π and σ orbitals have been omitted for clarity.

in Figure 4. The wave numbers for the peaks are provided in Table III. This vibrational structure results from excitation to excited vibrational states for the totally symmetric (A_{1g}) vibration of the excited electronic states. The separations of the peaks for both the ${}^3B_{1g}$ and the ${}^1A_{2g}$ transitions are $170 \pm 10 \text{ cm}^{-1}$. The vibrational wave number $\bar{\nu}_1$ for this A_{1g} vibration is somewhat smaller, as expected, than the 205 cm^{-1} reported by Hendra²² from the Raman spectrum of K_2PtBr_4 which, of course, will apply to the ground electronic state.

To this point there has been a very close correlation between the transitions of K_2PtBr_4 and K_2PtCl_4 . This feature is illustrated in Figure 5 where the band maxima energies for $15^\circ K$ spectra have been plotted for the two salts.

Up to the 1E_g transition the bands of K_2PtBr_4 have fallen $1500\text{--}2200 \text{ cm}^{-1}$ below the corresponding bands of K_2PtCl_4 . The character of the bands has been similar as well in that the same transitions have exhibited the vibrational structure. For both the salts the $d \leftarrow d$ transitions below $30,000 \text{ cm}^{-1}$ have considerably lower peak heights, are narrower, and accordingly have much lower oscillator strengths at the lower temperatures. These features are consistent with their ex-

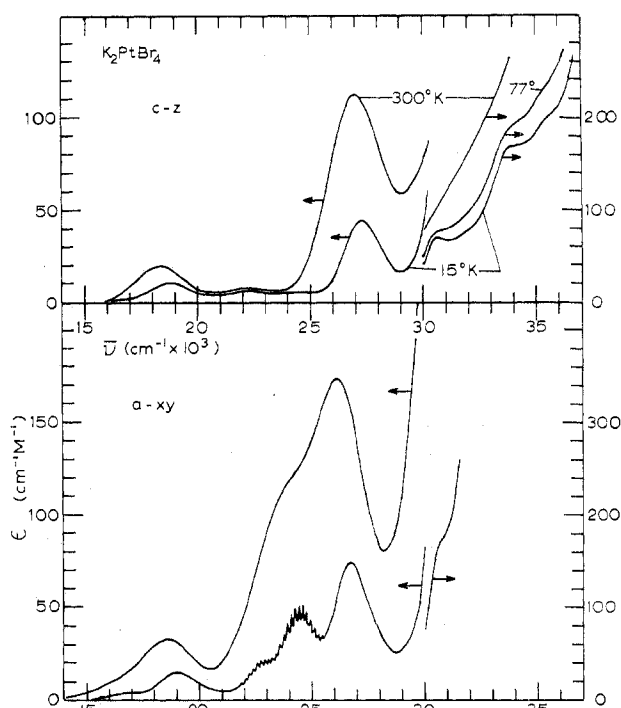


Figure 3. Polarized crystal spectra for K_2PtBr_4 . From 14,000 to 30,000 cm^{-1} the crystal was 26μ thick. Above 30,000 cm^{-1} the crystal was 11.5μ thick.

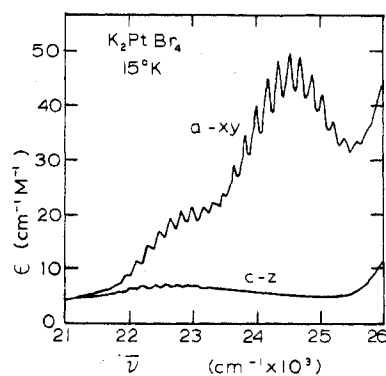
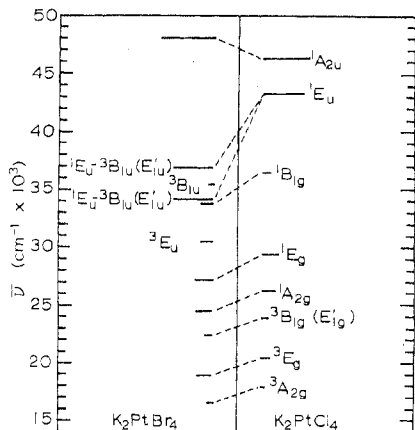


Figure 4. Section of the $15^\circ K$ spectrum for K_2PtBr_4 which exhibits vibrational structure. The crystal was 26μ thick.

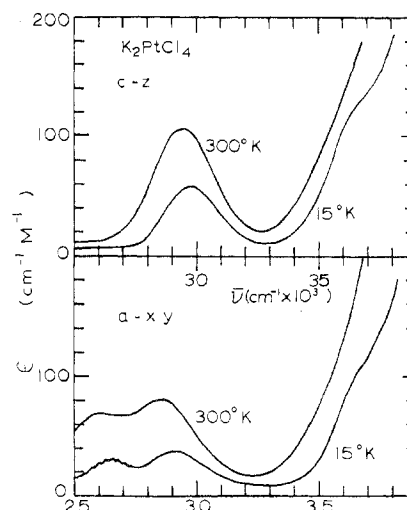
Table III. Energies ($\bar{\nu}$, cm^{-1}) for the Resolved Vibrational Peaks for the ${}^3B_{1g}(E'_{1g})$ and the ${}^1A_{2g}$ Transitions (15°K)

a polarizn		c polarizn (very weak)
21,720	23,810	22,050
21,900	23,980	22,220
22,080	24,150	22,400
22,260	24,330	22,570
22,440	24,520	22,760
22,620	24,690	22,930
22,800	24,870	23,090
22,970	25,040	23,270
23,140	25,220	
23,310	25,390	
23,480	25,560	
23,650	25,730	

**Figure 5.** Comparison for excited states of K_2PtBr_4 and K_2PtCl_4 . The length of line for each state is proportional to $\log \epsilon_{\text{max}}(15^\circ)$ for the crystal transitions and $\log \epsilon_{\text{max}}(\text{soln})$ for the intense transitions.

citation by the vibronic mechanism whereby asymmetric vibrations serve as perturbations to mix in asymmetric wave functions. One difference between the two salts has been the relative intensities for the alternate polarizations. For K_2PtCl_4 , bands in c - z polarizations were more intense than in a - x , y for the transition to 3E_g and 1E_g whereas the intensity ratios were reversed for K_2PtBr_4 . This feature implied that the 1E_u transition from which the $g \leftarrow g$ transitions were borrowing intensity in x , y polarization had moved to lower energy relative to the ${}^1A_{2u}$ transition which would provide intensity for z polarization.

The fourth spin-allowed transition for K_2PtCl_4 to the ${}^1B_{1g}$ state, $\sigma^*(b_{1g}) \leftarrow a_{1g}(d_{2z})$, has not previously been observed in a single-crystal spectrum. Assigned to this transition was a shoulder on a rapidly rising absorption at *ca.* $36,500 \text{ cm}^{-1}$ in solution²³ and in diffuse reflectance.²⁴ The thinnest crystal of K_2PtCl_4 used for our earlier spectral work⁷ was nearly 50μ thick. Since we have developed techniques to prepare routinely crystals about 10 – 20μ thick, a $15\text{-}\mu$ crystal of K_2PtCl_4 was prepared. The polarized spectra for this crystal are shown in Figure 6 where it can be seen that this band occurs in both polarizations at 15°K . The band in each polarization occurs on steeply rising absorption regions so its temperature dependence is not apparent. The transition does appear to be considerably weaker than the other spin-allowed $d \leftarrow d$ transitions at the low temperature, despite its proximity to the allowed transitions. The first bands above the 1E_g peak for K_2PtBr_4 lie at only $30,500$ (c) and $30,700$

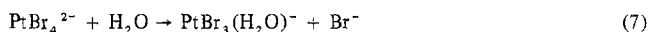
(23) J. Chatt, G. O. Gamlen, and L. E. Orgel, *J. Chem. Soc.*, 486 (1958).(24) P. Day, A. F. Orchard, A. J. Thompson, and R. J. P. Williams, *J. Chem. Phys.*, 42, 1947 (1965).**Figure 6.** Portions of the polarized crystal spectra at 300 and 15°K for a crystal of K_2PtCl_4 , 15μ thick.

cm^{-1} (a), some 6000 cm^{-1} below the band seen in K_2PtCl_4 . Since the $36,500\text{-cm}^{-1}$ assignment seems reasonable as ${}^1B_{1g}$ for K_2PtCl_4 in view of the component at $24,000 \text{ cm}^{-1}$ which must be assigned as ${}^3B_{1g}$, the K_2PtBr_4 band at $30,500 \text{ cm}^{-1}$ should not be assigned as ${}^1B_{1g}$ since the ${}^3B_{1g}$ component is only $1,300 \text{ cm}^{-1}$ below the corresponding K_2PtCl_4 band. The assignment of this $30,500\text{-cm}^{-1}$ band will be discussed with the high-energy transitions.

Allowed and High-Energy Transitions. In consideration of the high-energy states, it was noted that the aqueous solution spectrum provided a much better resolution for the band at *ca.* $24,000 \text{ cm}^{-1}$ than the a -polarization crystal spectrum where this band is seen only as a shoulder at 300° . However, the crystal yielded a deep valley with minima at $28,000$ – $29,000 \text{ cm}^{-1}$ in both polarizations. Such a minimum did not occur in the solution spectrum. It has been concluded that the solution component at $31,500 \text{ cm}^{-1}$ with an intensity, ϵ , of $600 \text{ cm}^{-1} M^{-1}$ either is not present in the crystal spectra or must have a much lower intensity. The possibility exists that this is an intense peak of a minor impurity or solution species. One possibility considered was that the sample contained PtBr_6^{2-} since its formation was observed in solutions standing for long periods from either air oxidation or an autoredox reaction. PtBr_6^{2-} has a broad peak,²⁵ ϵ $18,000 \text{ cm}^{-1} M^{-1}$, from $31,000$ to $33,000 \text{ cm}^{-1}$. Therefore a 3% content of PtBr_6^{2-} would yield such a component. However, this concentration would produce a higher absorbance at $25,000 \text{ cm}^{-1}$ than was observed. Therefore, the presence of PtBr_6^{2-} cannot account completely for the component.

Since the hydrazine reduction utilized for the preparation of K_2PtBr_4 might conceivably introduce amine-type ligands, the infrared spectrum from 600 to 3800 cm^{-1} was recorded for the anhydrous compound in a pressed KBr disk. The spectrum was clear of any absorption other than that which might be due to a trace of water over the entire region scanned. There were therefore no detectable absorptions of the possible N-H vibrations.

The PtBr_4^{2-} solution for the spectrum contained $1 M$ KBr to reduce the formation of $\text{PtBr}_3(\text{H}_2\text{O})^-$ and $\text{Pt}_2\text{Br}_6^{2-}$ by the reactions

(25) C. K. Jorgensen, *Acta Chem. Scand.*, 10, 518 (1956).

From equilibrium quotients for these reactions²⁶ the fraction of PtBr_4^{2-} converted into these species is calculated to be for $\text{PtBr}_3(\text{H}_2\text{O})^-$ 0.3% and for $\text{Pt}_2\text{Br}_6^{2-}$ 0.01%. It seems likely that these concentrations are too small to provide a band of this intensity. The Br^- might possibly form PtBr_5^{3-} with fivefold coordination, but Mason and Gray¹⁹ reported this spectral component in acetonitrile without an excess of bromide. Although Jorgensen²⁷ did not report the solution components at 31,500 and 34,200 cm^{-1} , he did note that the component at 27,000 cm^{-1} was seen only as a shoulder. Thus, although an impurity or solution species to account for this 31,500- cm^{-1} band cannot be ruled out unambiguously, some possible crystal effects to account for its absence will be discussed following the assignment of the high-energy transitions.

The solution spectrum for PtBr_4^{2-} exhibits three bands with increasing intensity at 34,200, 37,200, and 48,000 cm^{-1} . There has not been unanimity in the assignment of the intense high-energy bands for the platinum(II) complexes. A fully allowed transition in a D_{4h} system must be to either a ${}^1A_{2u}$ state for z polarization or to a 1E_u state for x, y polarization. Chatt, Gamlen, and Orgel,²³ Cotton and Harris,⁴ and McCaffery, Shatz, and Stephens²¹ have supported assignments of the intense bands of PtCl_4^{2-} as $6p \leftarrow 5d$ whereas Jorgensen,²⁷ Basch and Gray,³ and Mason and Gray¹⁹ have supported $M(\sigma^*) \leftarrow L(\pi)$ charge transfers. For PtCl_4^{2-} in solution there is a peak at 46,400 cm^{-1} (ϵ 11,000 $\text{cm}^{-1} M^{-1}$) with a shoulder at 43,400 cm^{-1} (ϵ 6,000 $\text{cm}^{-1} M^{-1}$). The $M(\sigma^*) \leftarrow L(\pi)$ charge transfer for a bromide ligand is expected to be at lower energy than for a chloride in an equivalent charge situation. Therefore Jorgensen and Gray with his co-workers have cited the low-energy 34,200 cm^{-1} and especially the 37,200- cm^{-1} bands of the solution spectrum in support of their assignments.

The ordering of states which can be predicted for the alternative assignments is somewhat different, as illustrated in Figure 7. For the $p_z \leftarrow d$ transitions the lowest ungerade spin-allowed transition will be to a ${}^1B_{1u}$ state ($p_z \leftarrow d_{xy}$) and therefore forbidden. The lowest allowed state will be 1E_u , $a_{2u}(p_z) \leftarrow e_g(d_{xz}, d_{yz})$, and hence will be a polarized for the crystal. Since ${}^1E_g(\sigma^* \leftarrow d)$ is 7000 cm^{-1} lower than ${}^1B_{1g}$, presumably the ${}^1A_{2u}(p_z \leftarrow d_{z^2})$ state should be expected a comparable distance above 1E_u ; although the exact separation may be modified by electron-electron repulsion energies. For the ligand π orbitals, the one-electron semiempirical molecular orbital calculations of Basch and Gray³ have placed the b_{2u} and the e_u orbitals very close together with the a_{2u} orbital only slightly below. Apparently, Cotton and Harris obtained a slightly greater separation in their orbital energies but unfortunately they did not label the orbitals in their tabulation of energies.⁴ The b_{2u} orbital, which is completely nonbonding, leads to the ${}^1A_{2u}$ state ($\sigma^*(b_{1g}) \leftarrow b_{2u}$). The e_u orbital, leading to the 1E_u state ($\sigma^*(b_{1g}) \leftarrow e_u$), is involved in bonding. However, it is an orbital of intermediate energy, between the metal $p_{x,y}$ orbitals and the ligand σ orbitals. Although the orbital may contain both σ and π character, its energy is rather effectively "pinned" close to the diagonal energy for the halide p orbitals in the secular equation. The a_{2u} orbital, which may be involved in out-of-plane π bonding, leads to a ${}^1B_{2u}$ state ($\sigma^*(b_{1g}) \leftarrow a_{2u}$), and its transition is therefore forbidden.

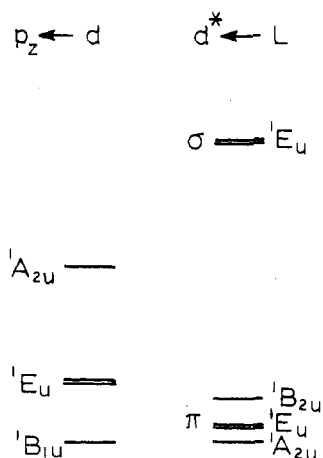


Figure 7. Ordering of ungerade excited states for alternate assignments.

For PtCl_4^{2-} , Schatz and his coworkers²¹ showed that there was an MCD A term associated with the shoulder at 43,400 cm^{-1} . No A term was evident for the 46,400 cm^{-1} peak which therefore could be assigned as ${}^1A_{2u}$. The band at the shoulder must contain a 1E_u component although a ${}^1A_{2u}$ component as well for the shoulder was not excluded.

From the crystal spectra, Figure 3, it can be seen that although the a -polarized absorbance has risen above a measurable value by 32,000 cm^{-1} at 15°K, the c -polarized spectrum was followed nearly to 37,000 cm^{-1} . Three weak transitions can be seen in c polarization between 30,000 and 36,000 cm^{-1} . It is possible to conclude therefore that the intense transitions at 34,200 and 37,200 cm^{-1} for the solution must be polarized in the x, y direction and that the first ${}^1A_{2u}$ transition can only be associated with the 48,000- cm^{-1} band. The very large separation between the intense x, y -polarized and z -polarized spectra in PtBr_4^{2-} and indeed an increase in the transition energy of ${}^1A_{2u}$ state from 46,400 to 48,000 cm^{-1} with a decrease in energy of two 1E_u states does not appear to be in agreement with either of the alternative assignments alone.

The following assignments are suggested to account for the experimental observations. For PtCl_4^{2-} the lower transition is essentially ${}^1E_u(p_z \leftarrow d_{xz}, d_{yz})$. However, the $M \leftarrow L(\pi)$ states are sufficiently close to ${}^1A_{2u}(p_z \leftarrow d_{z^2})$ that considerable mixing with the ${}^1A_{2u}(M \leftarrow L(\pi))$ transition by the electron-electron repulsion perturbation lowers the ${}^1A_{2u}$ energy significantly to provide a separation of only 3000 cm^{-1} between the ${}^1A_{2u}$ and the lower 1E_u states. For PtBr_4^{2-} the $p_z \leftarrow d$ state energies have moved higher whereas the $M \leftarrow L(\pi)$ energies have moved lower. Thus the ${}^1A_{2u}$ state at 48,000 cm^{-1} may be predominantly charge transfer whereas a strong interaction of 1E_u states has dropped their lower energy to about 35,500 cm^{-1} . In addition, for PtBr_4^{2-} there is not one but the two intense bands at 34,200 and 37,000 cm^{-1} in x, y polarization. The presence of two strong transitions could result from a near coincidence of a 1E_u state and a triplet state by virtue of the strong spin-orbit coupling of the heavy platinum atom. In the double group D'_4 the 1E_u state may be represented as a basis for the irreducible representation E'_{1u} , where the u refers to the orbital part only. Since the two-electron triplet functions transform as A'_2 and E'_1 , any orbitally asymmetric triplet state will contain E'_{1u} components. Possible suitable triplet states are ${}^3A_{2u}$ and the ${}^3B_{1u}(p_z \leftarrow d_{xy})$. Since the ${}^1A_{2u}$ state is so much higher, it is felt that ${}^3B_{1u}$ is the more likely. However, this will require considerable stabilization of 1E_u by virtue of the mixing of

(26) J. E. Teggin, D. R. Gano, M. A. Tucker, and D. S. Martin, Jr., *Inorg. Chem.*, **6**, 69 (1967).

(27) C. K. Jorgensen, U. S. Army Report DA-91-506-EUC, 1959, p 241.

the ($p_z \leftarrow d_{xz,yz}$) and the ($M(\sigma^*) \leftarrow L(\pi)$) components. With a near coincidence of the diagonal energies of $E'_{1u}(^1E_u)$ and $E'_{1u}(^3B_{1u})$ the two states will be split by about twice the off-diagonal spin-orbit coupling energy; and both will carry comparable intensities. The splitting of 3000 cm^{-1} between the bands at $34,200$ and $37,200\text{ cm}^{-1}$ appears reasonable for such spin-orbit splitting.

The weak band at $30,500\text{ cm}^{-1}$, which is seen in both a and c polarization, was considerably different in character from the vibronically excited $\sigma^* \leftarrow d$ transitions. For example, if its intensity had increased in a similar manner between 15 and 300°K , then it should have been clearly seen at 300°K in c polarization, at least. However, it cannot be discerned at all in the high-temperature scans. It has been concluded therefore that it is a weak but dipole-allowed transition whose intensity is insensitive to temperature changes. As the band narrows at low temperatures the peak height increases to maintain the same integrated intensity. It is proposed that the $30,500\text{-cm}^{-1}$ band therefore is the 3E_u transition. The 3E_u states possess a pair of E'_{1u} wave functions which mix with 1E_u states by virtue of the spin-orbit coupling to have an x, y -transition dipole moment. Its diagonal energy separation from the intense E'_{1u} states may be large enough that the intensity and energy shift are small however. Another of the six components of 3E_u will be A'_{2u} . This state will mix with $^1A_{2u}$ to obtain a z -transition dipole moment as well.

The weak transition seen at $33,800\text{ cm}^{-1}$ in z polarization is only 1700 cm^{-1} below the transition, assigned as $^1B_{1g}$ which is seen in K_2PtCl_4 . Since this is about the same separation of the other $\sigma^* \leftarrow d$ transition pairs which have been identified, the assignment of these transitions in the two salts as $^1B_{1g}(\sigma^* \leftarrow d_{z^2})$ seems reasonable. Finally, the very weak band seen at $35,300\text{ cm}^{-1}$ in c polarization may be the B'_{2u} component of $^3B_{1u}$. This transition would be vibronically allowed in this polarization by virtue of the perturbation by the B_{1g} vibration, a stretching mode. This state is the companion of the $^3B_{1u}$ triplet states which provides the intense band by mixing with 1E_u in the E'_{1u} representation. The presence of a vibronically allowed transition at just this energy supports the $^3B_{1u}$ assignment since the $^3A_{2u}$ is vibronically forbidden in z polarization.

The component resolved in the solution at $31,500\text{ cm}^{-1}$ ($\epsilon\ 600\text{ cm}^{-1} M^{-1}$) now deserves further comment. Its intensity is rather intermediate, much stronger than the $\sigma^* \leftarrow d$ transitions but much weaker than the two transitions at $34,200$ and $37,000\text{ cm}^{-1}$ which presumably have a large 1E_u component. It is suggested that this $31,500\text{-cm}^{-1}$ band is the transition to the E'_{1u} components of 3E_u . In that case it would be the same transition which appears at $30,500\text{ cm}^{-1}$ in the a polarization of the crystal with a very much lower intensity. In a crystal a transition can be shifted from a free ion value (in principle the gaseous state value) by the expression²⁸

$$\bar{\nu} = \bar{\nu}^0 + D + I \quad (9)$$

where $\bar{\nu}^0$ is the free ion transition energy, D is the difference in van der Waals energy between the excited-state and ground-state ions, and

$$I = \sum_{m \neq n} I_{mn} = \sum f \varphi'_m \varphi^0_n |V_{mn}| \varphi^0_m \varphi'_n d\tau \quad (10)$$

where φ^0 and φ' are the molecular wave functions for the ground state and excited state ions, respectively, and n and m

are indices for the molecules. The quantity D does not depend upon the intensity whereas I is intensity dependent. The rather good agreement between the wave numbers for the low intensity bands in the solution and crystal indicates that solution effects and the D terms do not cause large shifts in the transition energies. The I_{mn} terms are frequently approximated by the classical interaction of transition dipole moments between the two molecular species.²⁹ The transition moment for the $37,200\text{ cm}^{-1}$ band in the solution spectrum was calculated to be 0.65 \AA from the oscillator strength by the equation

$$f = 1.085 \times 10^{-5} \bar{\nu}(2/3) |\chi'|^2 \quad (11)$$

where χ' is transition moment, \AA , and the factor $2/3$ arises from the random orientation of molecules with two transitions polarized x and y , respectively. The transition moment interaction yields for I_{mn} the expression

$$I_{mn} = |\chi'|^2 e^2 R_{mn}^{-3} (1 - 3 \cos^2 \theta) \quad (12)$$

where R_{mn} is the distance between the ions n and m and θ is the angle between the vector R_{mn} and the x axis. A sum of I_{mn} over all the $PtBr_4^{2-}$ ions within a 50-\AA radius gave a value for I which was $+1000\text{ cm}^{-1}$ for the $37,200\text{-cm}^{-1}$ band. Intensities for transitions which mix with and therefore borrow from the $^1E_u \leftarrow ^1A_{1g}$ transitions are strongly dependent upon their separations from the first intense band. It seems possible therefore that an increase in the separations from the intense bands by the order 1000 cm^{-1} might reduce the intensity of the $31,500\text{-cm}^{-1}$ band to the much weaker $30,500\text{-cm}^{-1}$ band that was well resolved in the low-temperature crystal spectra. It was also demonstrated from similar computation that if the transition at $37,200\text{ cm}^{-1}$ occurred in z polarization, it would have been red-shifted by 2000 cm^{-1} . Hence the absence of a strong absorption in c polarization cannot be explained by a crystal shift of a z -polarized transition beyond the range of measurements.

The assignments for the transitions in accordance with the above discussions have been included in Table II. Admittedly, a number of the assignments are somewhat speculative. For both K_2PtCl_4 and K_2PtBr_4 the ordering of the d orbitals indicates a strong σ bonding to give the high $\sigma^*(b_{1g})$ orbitals. However, the splitting of the $b_{2g}(d_{xy})$ orbital and the $e_g^-(d_{xz-yz})$ orbitals indicates moderate π bonding as well. The $a_{1g}(d_{z^2})$ orbital is so low that the transition to the $^1B_{1g}$ state, $\sigma^* \leftarrow d_{z^2}$, lies among the allowed transitions for $PtBr_4^{2-}$. The fairly uniform difference between the $\sigma^* \leftarrow d$ transitions of $PtBr_4^{2-}$ and $PtCl_4^{2-}$ is quite striking. The difference between the intense transitions of the two ions therefore is somewhat surprising. For $PtCl_4^{2-}$ there appears to be a strong $^1A_{2u}$ transition close to the lowest 1E_u . The evidence consists of the rapid rise in absorption in both c and a polarization for K_2PtCl_4 and the MCD results of Schatz and co-workers.²¹ However, for $PtBr_4^{2-}$ any $^1A_{2u}$ transition lies at least $11,000\text{ cm}^{-1}$ above the lowest 1E_u . These results also provide rather good evidence for the "spin-forbidden" transitions in the form of the second strong band in x, y polarization separated by a reasonable spin-orbit interaction and the evidence for the weak but dipole-allowed 3E_u transitions in both x, y and z polarization. It seems that the intense transitions probably cannot be described simply as either charge transfer ($M \leftarrow L$) or as $6p \leftarrow 5d$, but probably with some mixing of both. Apparently, the electron-electron interactions

(28) D. P. Craig and S. H. Walmsley, "Excitons in Molecular Crystals," W. A. Benjamin, New York, N. Y., 1968, p 54.

(29) Reference 28, pp 59, 67.

as well as the spin-orbit coupling effects are important in determining transition energies and intensities.

Registry No. K₂PtBr₄, 13826-94-3.

Supplementary Material Available. A listing of structure factor amplitudes will appear following these pages in the microfilm edition

of this volume of the journal. Photocopies of the supplementary material from this paper only or microfiche (105 × 148 mm, 24× reduction, negatives) containing all of the supplementary material for the papers in this issue may be obtained from the Journals Department, American Chemical Society, 1155 16th St., N.W., Washington, D. C. 20036. Remit check or money order for \$3.00 for photocopy or \$2.00 for microfiche, referring to code number INORG-74-1366.

Contribution from the Department of Chemistry,
University of Missouri, Columbia, Missouri 65201

Structure of *trans*-Chloro(methylimido)tetrakis(methylamine) rhenium(V) Perchlorate

R. S. SHANDLES, R. K. MURMANN, and E. O. SCHLEMPER*

Received September 12, 1973

AIC30678M

The crystal structure of the *trans*-chloro(methylimido)tetrakis(methylamine)rhenium(V) ion, [Re(CH₃NH₂)₄(CH₃N)Cl]²⁺, has been determined as its perchlorate salt, using scintillation counter techniques in a three-dimensional X-ray diffraction study. The compound crystallizes in the orthorhombic space group *Pnam* with unit cell dimensions $a = 16.908$ (4) Å, $b = 8.641$ (2) Å, and $c = 12.759$ (5) Å. The density of 2.045 (1) g/cm³ calculated on the basis of four formula units per unit cell is in agreement with the flotation density of 2.01 (2) g/cm³. The structure was resolved by Patterson and Fourier methods and refined by full-matrix least-squares treatment to a conventional *R* factor of 4.1% using 1066 independent reflections. The perchlorate ion is disordered. The rhenium is octahedrally coordinated with a chlorine and five nitrogens. The Re-Cl distance is 2.403 (5) Å. The methylimido group is *trans* to the Cl with the Re-N(imido) distance 1.694 (11) Å and the N(imido)-C distance 1.46 (2) Å. The Cl-Re-N(imido)-C grouping is linear; Cl-Re-N = 179.4 (6)^o and Re-N-C = 180 (2)^o. The remaining four amine nitrogens are arranged in a plane around the rhenium with the metal above the plane toward the imido nitrogen. The average Re-N(amine) distance is 2.18 (2) Å. The average N(imido)-Re-N(amine) angle is 95.4 (7)^o. The rates of Cl⁻ hydrolysis and isotopic exchange in dilute HCl solution are compared.

Introduction

Considerable interest has been developing in the nature of rhenium-ligand multiple bonds which are often found in complex compounds. Usually the metal is in a high oxidation state and is bonded through nitrogen¹ or oxygen^{2,3} atoms. While there is no question as to which atoms are involved in these short bonds, as observed in crystal structure studies, there remains considerable doubt as to "normal distances" for single, double, and triple bonds.

This paper reports the structure of *trans*-chloro(methylimido)tetrakis(methylamine)rhenium(V) perchlorate. Previous work on this compound³ gave its preparation and identified its basic molecular structure by nmr means. It was found that the rhenium(V) is coordinated to an imino nitrogen and four amine nitrogens of methylamine and that the coordinated chloride ion is *trans* to the methylimine. The compound thus gives the unique opportunity to compare the geometrical parameters of CH₃-NH₂ with those of CH₃-N while both are bonded to the same rhenium(V) ion. Also of interest is the kinetics of the substitution process involving the coordinated Cl⁻ *trans* to the multiple-bonded imine. This structure allows a comparison of the substitution and isotopic exchange parameters with bond distances in this and similar complexes.

Experimental Section

Crystal Preparation. [Re(CH₃NH₂)₄(CH₃N)Cl](ClO₄)₂ was prepared as previously described³ and recrystallized from an acetone-water solution by the slow evaporation of solvent. The deep blue crystals were in the form of elongated octahedra.

X-Ray Data Collection. Precession photographs indicated an

orthorhombic cell. The systematic extinctions observed on these photographs were h odd for $h0l$ and $k + l$ odd for $0kl$. Thus the compound is either in the centrosymmetric space group *Pnam*, in which mirror symmetry is present, or the noncentrosymmetric space group *Pna2*₁. Standard optical goniometric methods established the eight faces of the crystal to be 101, 10 $\bar{1}$, $\bar{1}01$, $\bar{1}0\bar{1}$, 210, 2 $\bar{1}0$, $\bar{2}10$, and $\bar{2}\bar{1}0$. Decomposition in the X-ray beam was observed and thus the data collection time was kept minimal. The crystal used for the intensity measurements had the dimensions 0.08 mm × 0.06 mm × 0.11 mm, small enough so that absorption corrections could be made with a reasonable degree of accuracy. The crystal was aligned on a Picker programed four-circle diffractometer with the c -axis coincident with the ϕ axis of the diffractometer. Twenty-five intense reflections found on the preliminary photographs were accurately centered using Mo K α radiation (λ 0.7107 Å). From the setting angles found for these 25 reflections, the cell constants determined by a least-squares⁴ refinement were $a = 16.908$ (4) Å, $b = 8.641$ (2) Å, and $c = 12.759$ (5) Å. The calculated density based on four formula units per unit cell was 2.045 (1) g/cm³ which agrees with the experimental value of 2.01 (2) g/cm³ determined by flotation. The above refinement was used to calculate the setting angles for all reflections. The intensities were measured with a scintillation detector linear to greater than 8000 counts/sec. The intensities of 2272 reflections were measured out to a 2θ angle of 45^o, using Mo K α radiation filtered through a 1-mil niobium foil in front of a 3 mm × 3 mm receiving aperture. The takeoff angle was 2.0^o. A scan rate of 1.0^o/min was used for the variable 2θ scan. This scan was taken from 0.19^o below the 2θ setting for K α_1 (λ 0.70926 Å) to 0.31^o above the 2θ setting for K α_2 (λ 0.71354 Å). Stationary-background counts of 20 sec were taken at both ends of the scan. One-mil brass foils were used for attenuation to prevent exceeding 8000 counts/sec. The precalibrated foils gave attenuation factors of about 3. Three reflections chosen as standards were measured every 50 reflections

(4) All calculations were performed on the IBM 360/65 computer of the University of Missouri Computer Research Center using the following programs: W. Hamilton and J. A. Ibers, NUPIK, Picker input program; W. Hamilton, HORSE, general absorption program; R. Doedens and J. A. Ibers, NUCLS, least-squares program and a modification of W. R. Busing and H. A. Levy's ORFLS program; A. Zalkin, FORDAP, Fourier program; C. Johnson, ORTEP, thermal ellipsoid plot program; J. A. Ibers, FINDH, tetrahedral atom placement program.

(1) J. Chatt, J. R. Dilworth, and G. J. Leigh, *J. Chem. Soc. A*, 2239 (1970), and references therein.

(2) R. Shandles, E. O. Schlemper, and R. K. Murmann, *Inorg. Chem.*, 10, 2785 (1971), and references therein.

(3) R. Shandles and R. K. Murmann, *J. Inorg. Nucl. Chem.*, 27, 1869 (1965).